# Supporting Information

Oláhová *et al.* 10.1073/pnas.0805507105

## SI Materials and Methods

**Maintenance of Nematodes.** All animals were maintained by using standard methods on NGM-Lite agar (1, 2). *skn-1* (*zu67*)-containing lines were maintained by picking unc (heterozygotes) worms. Animals homozygous for *skn-1* (*zu67*) were identified as nonunc. *skn-1* (*zu67*) *gcs-1*::*GFP* animals homozygous for *skn-1* (*zu67*) were identified as nonunc rollers (which was later confirmed by their inability as adults to produce viable progeny, laying only dead eggs).

**Plasmid Construction.** The *prdx-2* ORF including the stop codon was amplified from *C. elegans* cDNA and cloned into pL4440 or *pPD95.75-Pges-1*::*GFP* (3) to generate pL4440+*prdx-2* or *pPD95.75-Pges-1*::*PRDX-2*. *pPD95.75-Pges-1*::*PRDX-2*$^{C170S}$ was created by replacing a 593-bp SalI/BamHI fragment from *pPD95.75-Pges-1*::*PRDX-2* with an equivalent fragment encoding the C170S substitution.

**Generation of New *C. elegans* Strains Used in These Studies.** VE1, homozygous for *prdx-2* (*gk169*), was made by backcrossing VC289 (CGC) (4) six times with N2. LD1172 (N2 *gcs-1*::*GFP*) was made by UV-induced integration of extra-chromosomal *gcs-1*::*GFP* array, marked with *rol-6* (5). *prdx-2 gcs-1*::*GFP* (VE4) was generated by breeding VE1 and LD1172. *skn-1* (*zu67*) *gcs-1*::*GFP* (LD1173) was generated by breeding *skn-1* (*zu67*) animals with LD1172. Transgenic animals containing *eavEx1Pges-1*::*prdx-2* line 1 (VE5) and line 2 (VE6) or *eavEx2Pges-1*::*prdx-2*$^{C170S}$ line 1 (VE10) and line 2 (VE11) were generated by coinjection of 80 ng/$\mu$l of either *pPD95.75-Pges-1*::*PRDX-2* or *pPD95.75-Pges-1*::*PRDX-2*$^{C170S}$ with 100 ng/$\mu$l pRF4 expressing the dominant *rol-6* injection marker, and 20 ng/$\mu$l pBluescript (total DNA concentration 200 ng/$\mu$l) into the gonad of adult wild-type (N2) worms (6). $F_1$ worms carrying transgenes were selected on the basis of the roller phenotype, plated individually, and maintained until the lines were established. *prdx-2* (*gk169*) *Pges-1*::*PRDX-2* line 1 (VE7), line 2 (VE8), and line 3 (VE9) were made by breeding VE5 with VE1.

**Synchronicity of Nematodes.** Recently starved animals arrested at L1 stage were washed off the plate by using 2 ml of M9 buffer, and the M9/worm suspension was transferred to a 15-ml polypropylene tube. Any adult animals were separated by allowing worms to sediment for 2–3 min, and supernatant containing L1 worms was then transferred to a fresh tube. The number and synchronicity of the L1 suspension was determined by counting the number of worms in 10 $\mu$l of suspension. The appropriate volume of the worm suspension was transferred onto seeded NGM-Lite plates to allow resumption of normal development.

**Viability Assays.** Well-fed L4-stage hermaphrodites were transferred to plates containing the indicated concentrations of $H_2O_2$ or sodium arsenite and incubated at 15 °C, unless otherwise indicated. The viability of each animal was assessed at the indicated times by microscopic examination for evidence of either pharyngeal pumping or movement in response to gentle prodding. Dead worms were counted and removed from plates. To assess the effect of PRDX-2 oxidation on stress resistance, larval L4-stage animals were washed from plates with either M9 buffer or M9 containing 5.0 mM $H_2O_2$, gently agitated at room temperature for 5 min, then washed twice with M9 buffer before transfer to plates containing the indicated concentrations of stress agents. Viability was then monitored as above.

**Statistical Analysis of Data.** In lifespan and viability assays, log-rank analysis (Minitab15) was used to determine whether differences between groups were significant. Cox's linear regression (SPSS15) methods were used to analyze data from multiple experiments.

**Peroxiredoxin Antibodies.** Rabbit polyclonal antibodies were generated against peptides based on the 16 amino acids at the carboxyl terminus of either PRDX-2 (anti-PRDX-2) or PRDX-3 (anti-PRDX-3) and affinity-purified against the same peptides (Eurogentec).

**Analysis of PMK-1 Phosphorylation.** Synchronized L4 nematodes (3,000–4,000) were washed from NGM-Lite plates with 5 ml of M9 buffer containing the indicated concentrations of sodium arsenite, incubated with gentle agitation (70 rpm) at room temperature for the indicated time, harvested by centrifugation at 32 $\times$ *g* for 1 min, then frozen in liquid nitrogen. Worm pellets were homogenized in 200 $\mu$l of lysis buffer [50 mM Tris·HCl, pH 7.5; 150 mM NaCl; 0.5% (vol/vol) Nonidet P-40; 2 $\mu$g/ml pepstatin A; 2 $\mu$g/ml leupeptin; 100 mg/ml phenylmethylsulfonyl fluoride; 1% (vol/vol) aprotinin; 50 mM NaF] with 0.5-mm glass beads and a Mini Beadbeater (Biospec Products). Appropriate volumes of 4$\times$ sample buffer [0.5% bromophenol blue; 10% SDS; 625 mM Tris·HCl, pH 6.8; 50% (vol/vol) glycerol; 10% (vol/vol) 2-mercaptoethanol] were added to equal amounts of protein (3–10 $\mu$g). Denatured protein samples were then separated by SDS/PAGE and examined by Western blotting using rabbit polyclonal anti-phospho-p38 antibodies (New England Biolabs), followed by HRP-conjugated anti-rabbit IgG and ECL to determine PMK-1 phosphorylation. The membrane was stripped in 4.0% SDS and 62.5 mM Tris·HCl (pH 6.7) for 30 min at 50 °C, then reanalyzed by using anti-$\beta$-tubulin (E7; Developmental Studies Hybridoma Bank, University of Iowa, Iowa City) and HRP-conjugated anti-mouse IgG and ECL to confirm that blots were evenly loaded. Anti-PMK-1 antibodies were used to determine that total levels of PMK-1 were unaffected by loss of PRDX-2 (7).

**Measurements of *C. elegans* Aging.** ***Lipofuscin.*** Synchronized animals maintained on live *Escherichia coli* OP50 at 15 °C were examined for gut autofluorescence (lipofuscin) at 3 and 5 days of adulthood after excitation at 450–490 nm by using a Zeiss Axioskop 2 microscope (10$\times$ magnification). Lipofuscin levels were quantified essentially as described previously (8, 9). Images were captured under identical conditions, including exposure, by using a digital camera and Axiovision 3.1. The amount of gut autofluorescence was quantified by using Axiovision 3.1 software; the anterior part of the intestine was outlined in each image to define similar areas ($\pm$10%) for which the mean pixel value (brightness) was determined. The mean pixel value for the anterior intestine of day-old wild-type (N2) animals, in which no gut autofluorescence was visible, was also determined and used as a background value; i.e., this value was subtracted to give mean gut autofluorescence (lipofuscin) for each animal.

***Motility.*** The motility of 35–40 synchronized animals maintained on live *E. coli* OP50 at 15 °C on separate plates was assessed by recording the number of body lengths of sinusoidal movement over a 10-s period after gentle tapping of the plate. The body

movement span for each animal was determined as the first day on which an animal moved <0.25 body length during the 10-s period.

**Immunostaining.** Well-fed mixed-stage worms were fixed with 1% paraformadehyde and immunostained with anti-PRDX-2 antibodies by using established methods (10). Fixed animals were incubated with a primary anti-PRDX-2 antibody (1:1,000 dilution) overnight at 4 °C and subsequently incubated with an anti-rabbit secondary antibody (conjugated with Alexa Fluor 488) for 1 h at room temperature. Stained worms were fixed on microscope slides and costained with DAPI. Images were captured by using a Zeiss Axioskop 2 microscope and Axiovision imaging system. For embryo immunostaining, embryos were mounted on a poly(L-lysine)-coated microscope slide, fixed in −20 °C methanol for 20 min, washed twice in 1× PBS for 10 min, and immunostained as described above. The absence of staining in *prdx-2* (*gk169*) (VE1) null animals was used to confirm specificity of embryonic, larval, and adult staining patterns.

***prdx-2* RNA Interference.** ***Microinjection.*** *prdx-2* dsRNA was prepared by using Ambion's MEGAscript RNAi Kit and a *prdx-2* template generated by PCR (primer sequences available on request) from wild-type genomic DNA. RNA (1.5 $\mu$g/$\mu$l) was injected into young adult hermaphrodites by using standard microinjection methods (11). After injection the animals were transferred back to plates and incubated at 15 °C for at least 6 h before transfer to separate plates. Injected worms were moved to fresh plates every 24 h until they finished laying eggs.

***Feeding.*** HT115 *E. coli* containing either pL4440 or pL4440 containing the *prdx-2* ORF were grown to $OD_{600}$ = 1 in LB containing 50 $\mu$g/ml ampicillin and 10 $\mu$g/ml tetracycline. RNA expression was induced by addition of 1 mM isopropyl $\beta$-D-thiogalactopyranoside (IPTG), then the *E. coli* were used to seed plates containing 0.3% (wt/vol) NaCl, 1.7% (wt/vol) agarose, 0.25% (wt/vol) Bactopeptone, 0.08% (wt/vol) yeast extract, 1.0 mM $CaCl_2$, 1.0 mM $MgSO_4$, 2.5 mM phosphate buffer (pH 6.0), 1.0 mM IPTG, 5 $\mu$g/ml cholesterol, and 60 $\mu$g/ml ampicillin. Plates were dried for 2 days at room temperature before use.


1. Brenner S (1974) The genetics of *Caenorhabditis elegans*. *Genetics* 77:71–94.
2. Sun AY, Lambie EJ (1997) gon-2, a gene required for gonadogenesis in *Caenorhabditis elegans*. *Genetics* 147:1077–1089.
3. Inoue H, *et al*. (2005) The *C. elegans* p38 MAPK pathway regulates nuclear localization of the transcription factor SKN-1 in oxidative stress response. *Gene Dev* 19:2278–2283.
4. Isermann K, *et al*. (2004) A peroxiredoxin specifically expressed in two types of pharyngeal neurons is required for normal growth and egg production in *Caenorhabditis elegans*. *J Mol Biol* 338:745–755.
5. An JH, Blackwell TK (2003) SKN-1 links *C. elegans* mesendodermal specification to a conserved oxidative stress response. *Gene Dev* 17:1882–1893.
6. Mello CC, *et al*. (1991) Efficient gene transfer in *C. elegans*: Extrachromosomal maintenance and integration of transforming sequences. *EMBO J* 10:3959–3970.
7. Kim DH, *et al*. (2002) A conserved p38 MAP kinase pathway in *Caenorhabditis elegans* innate immunity. *Science* 297:623–626.
8. Boehm M, Slack F (2005) A developmental timing microRNA and its target regulate life span in *C. elegans*. *Science* 310:1954–1957.
9. Chavez V, Mohri-Shiomi A, Maadani A, Vega LA, Garsin DA (2007) Oxidative stress enzymes are required for DAF-16-mediated immunity due to generation of reactive oxygen species by *Caenorhabditis elegans*. *Genetics* 176:1567–1577.
10. Finney M, Ruvkun G (1990) The unc-86 gene product couples cell lineage and cell identity in *C. elegans*. *Cell* 63:895–905.
11. Fire A, *et al*. (1998) Potent and specific genetic interference by double-stranded RNA in *Caenorhabditis elegans*. *Nature* 391:806–811.

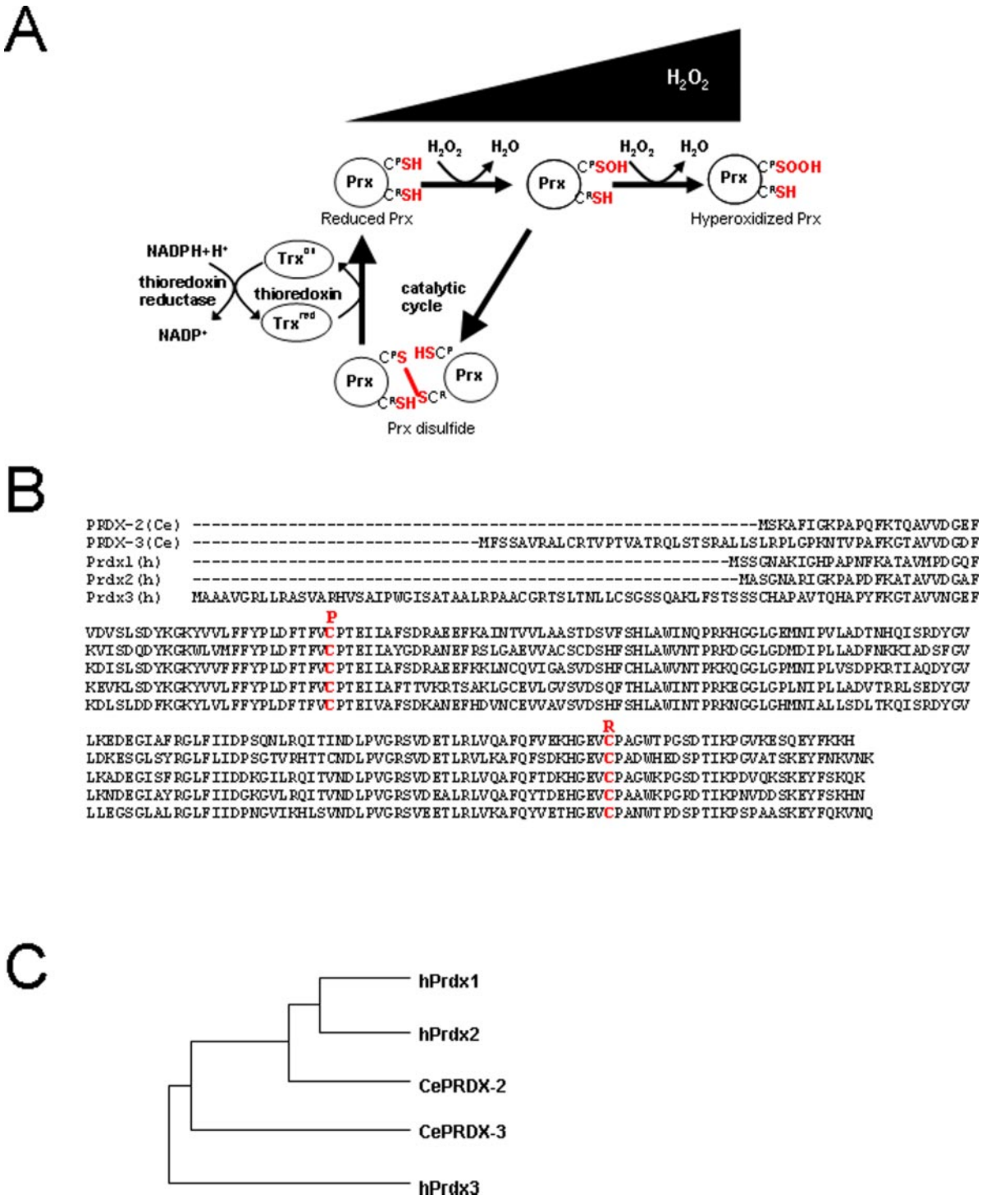


**Fig. S1.** The catalytic mechanism of 2-Cys Prx such as the *C. elegans* Prx, PRDX-2 and PRDX-3. (*A*) The catalytic breakdown of hydrogen peroxide by the thioredoxin peroxidase activity of typical 2-Cys Prx involves the formation of a disulfide between peroxidatic ($C^P$) and resolving ($C^R$) cysteines in neighboring Prx molecules (Prx disulfide). The Prx disulfide is reduced by thioredoxin to regenerate reduced Prx. Oxidized thioredoxin ($Trx^{ox}$) is reduced by thioredoxin reductase using NADPH to regenerate reduced thioredoxin ($Trx^{red}$). The thioredoxin peroxidase activity of Prx is inactivated by hyperoxidation of the peroxidatic cysteine from sulfenic (SOH) to sulfinic acid (SOOH) at higher concentrations of hydrogen peroxide. (*B* and *C*) The *C. elegans* genome encodes two 2-Cys Prx, PRDX-2 and PRDX-3. (*B*) Primary sequence alignment (ClustalW) showing the relationship between *C. elegans* (Ce) PRDX-2 (NP872052), PRDX-3 (NP497892), and human (h) 2-Cys Prx Prdx1 (CAG28580), Prdx2 (CAG29352), and Prdx3 (CAG29340). Peroxidatic (P) and resolving (R) cysteines are indicated in red. (*C*) Phylogenetic (Phylip) analysis identifies PRDX-2 as the most probable ortholog of the tumor suppressor Prdx1, whereas PRDX-3 contains a putative mitochondrial leader sequence and is more closely related to the mitochondrial family of Prx (represented here by hPrdx3).

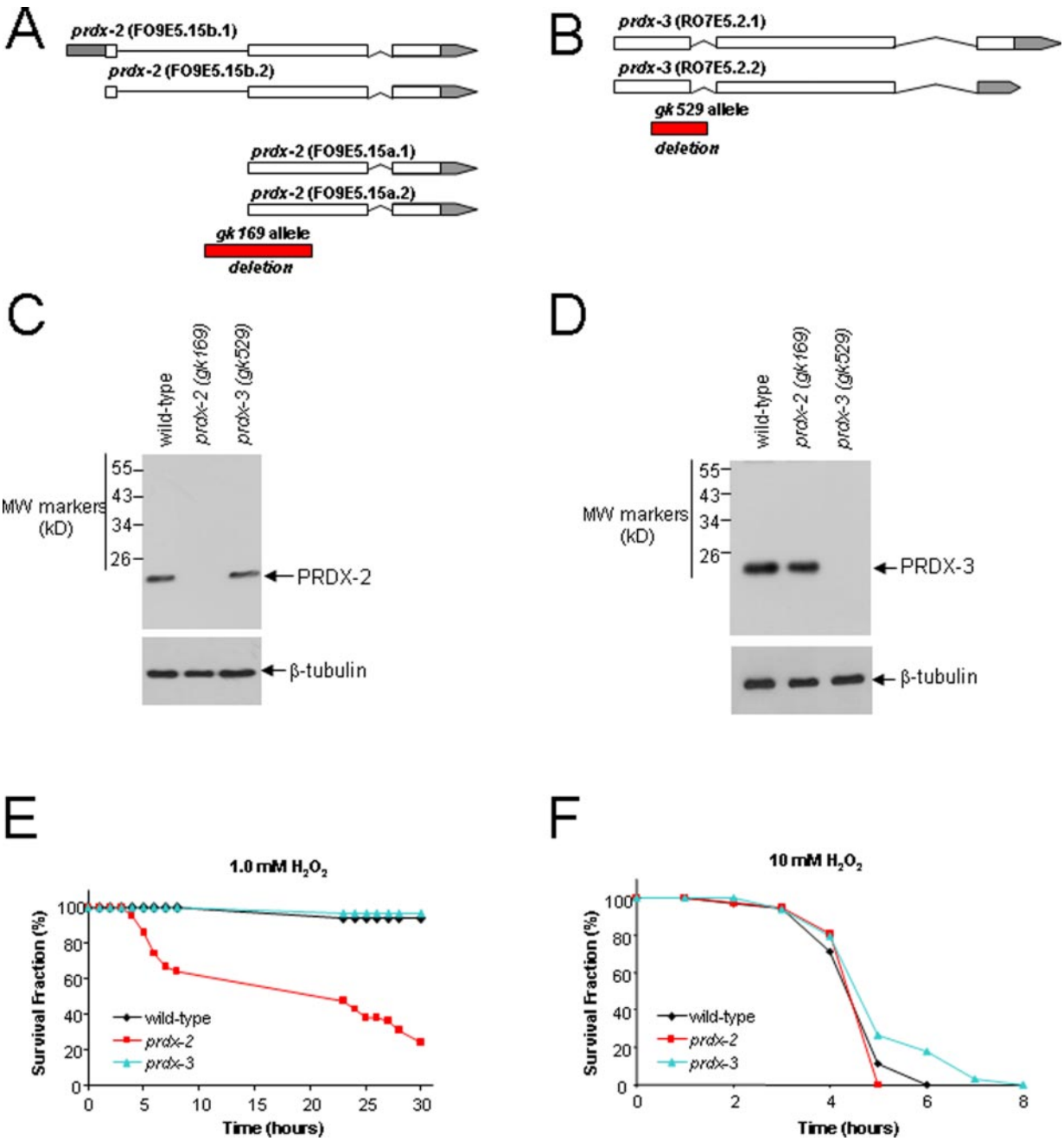


**Fig. S2.** PRDX-2, but not PRDX-3, is important for protection against hydrogen peroxide toxicity. (*A–D*) PRDX-2 and PRDX-3 are absent from animals containing the *gk169* or the *gk529* allele, respectively. (*A*) *prdx-2* (*gk169*) and (*B*) *prdx-3* (*gk529*) *C. elegans* mutants contain predicted null alleles. Exons are indicated in white, untranslated regions in gray, and deletions in red. (*C* and *D*) The absence of PRDX-2 and PRDX-3 proteins from *prdx-2* (*gk169*) and *prdx-3* (*gk529*) mutants was confirmed by Western blot analysis of proteins extracted from wild-type (N2), *prdx-2* (*gk169*), and *prdx-3* (*gk529*) mutant animals and separated under reducing conditions (denatured in sample buffer containing 2-mercaptoethanol). (*C*) Anti-PRDX-2 antibodies detected a single protein with a mobility consistent with the predicted size for PRDX-2 (21.8 kDa) that is absent from *prdx-2* (*gk169*) mutants. (*D*) Anti-PRDX-3 antibodies detected a protein with a mobility consistent with the predicted size for PRDX-3 (24.9 kDa) that is absent from *prdx-3* (*gk529*) mutants. Antibodies to β-tubulin were used as a loading control. (*E*) *prdx-2* (*gk169*) mutant animals are more sensitive to 1.0 mM hydrogen peroxide than wild-type (N2) or *prdx-3* (*gk529*) animals (log-rank test on *prdx-2* compared with wild type, $P < 0.0001$). (*F*) At higher concentrations (10 mM) of hydrogen peroxide, wild-type (N2), *prdx-2* (*gk169*), and *prdx-3* (*gk529*) mutant animals have similar sensitivities. The viability of wild-type (N2), *prdx-2* (*gk169*), and *prdx-3* (*gk529*) animals was monitored on plates containing the indicated concentrations of hydrogen peroxide. These experiments were repeated several times with similar results. Representative experiments are shown in which there are at least 30 animals in each group.

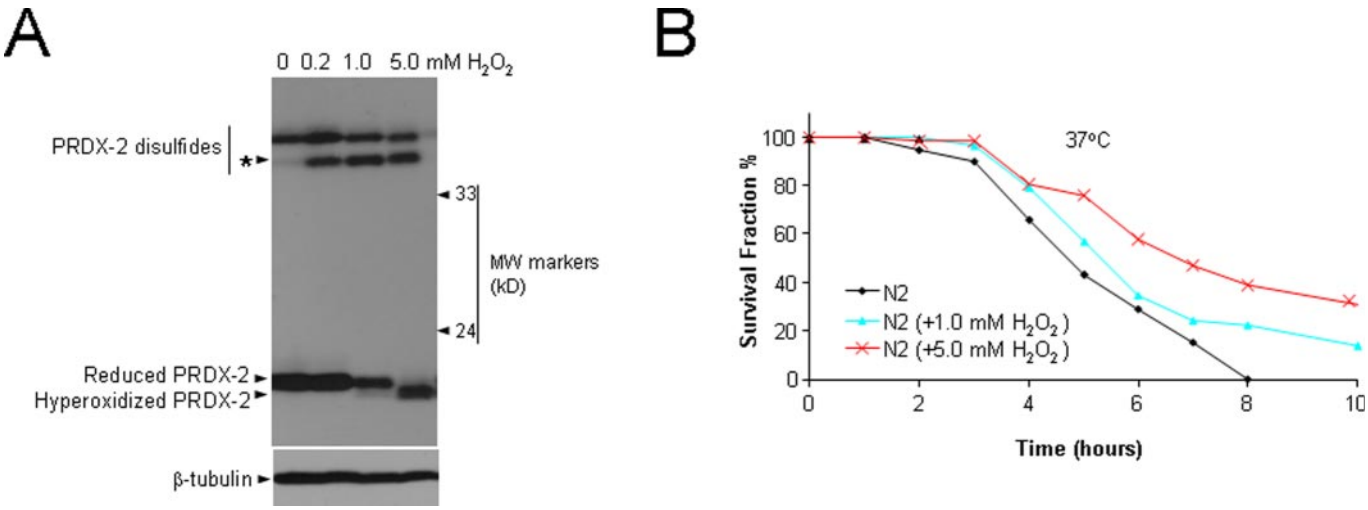


**Fig. S3.** Pretreatment of wild-type (N2) worms with sufficient hydrogen peroxide to generate substantial levels of hyperoxidized PRDX-2 (5.0 mM $H_2O_2$) extends survival at 37 °C more effectively than pretreatment with a lower concentration (1.0 mM $H_2O_2$), at which minimal amounts of PRDX-2 are hyperoxidized. (*A*) Analysis of the redox status of PRDX-2 in wild-type (N2) worms treated for 5 min with the indicated concentrations of $H_2O_2$ shows that PRDX-2 becomes increasingly oxidized after exposure to increasing concentrations of hydrogen peroxide. Nonreducing Western blot analysis of protein samples, treated with the thiol-reactive agent AMS, allows electrophoretic separation of reduced, hyperoxidized PRDX-2 and PRDX-2 disulfide dimers (PRDX-2 disulfide) (Fig. S1*A*). In untreated animals, PRDX-2 is present as a reduced monomer and a higher molecular weight form (PRDX-2 disulfide). The mobility of this high molecular weight form and its absence from samples run under reducing conditions (Fig. S2*C*) are consistent with it being produced by PRDX-2 disulfide dimer, a catalytic cycle intermediate (Fig. S1*A*). Exposure to 0.2 mM and 1.0 mM $H_2O_2$ leads to formation of an additional $H_2O_2$-induced PRDX-2 disulfide (*), but substantial amounts of reduced PRDX-2 remain. However, PRDX-2 is completely oxidized to disulfide and hyperoxidized monomeric forms after treatment with 5.0 mM $H_2O_2$. $\beta$-Tubulin is the loading control. (*B*) When the viability of worms, pretreated for 5 min with M9 containing different concentrations of $H_2O_2$, was monitored at 37 °C, it was found that only pretreatment with 5.0 mM $H_2O_2$ conferred significant protection against heat stress. This experiment was repeated 3 times, giving similar results. Although treatment with 1.0 mM $H_2O_2$ slightly increased thermal tolerance, this increase was not statistically significant. [Cox's linear regression: N2 vs. N2 + 5.0 mM $H_2O_2$ ($P = 0.001$), N2 vs. N2 + 1.0 mM $H_2O_2$ ($P = 0.374$)]. A representative experiment is shown in which there were 58–79 animals in each group. Together, these data are consistent with a role for hyperoxidized PRDX-2 and not PRDX-2 disulfides in $H_2O_2$-induced protection against heat stress.

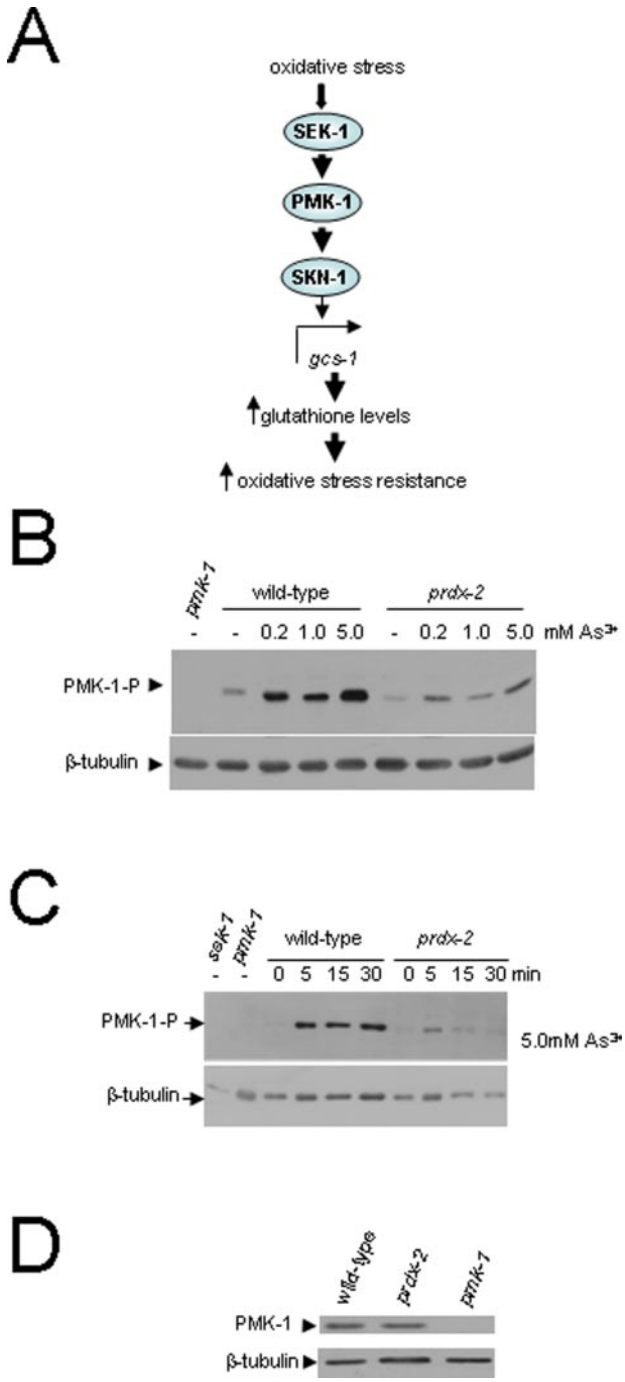


**Fig. S4.** PRDX-2 is required for arsenite-induced activation of a conserved p38-related MAPK signaling pathway important for phase II gene expression (including *gcs-1*) and oxidative stress resistance. (*A*) The activation of the MAPKK SEK-1 leads to activation of the PMK-1 MAPK by phosphorylation. The SKN-1 transcription factor is phosphorylated by PMK-1, allowing it to accumulate in the nucleus of intestinal cells, where it activates target-gene expression, including *gcs-1* encoding γ-glutamyl cysteinyl synthetase heavy chain (GCS-1). GCS-1 catalyzes the rate-limiting step in glutathione synthesis. Thus, increased GCS-1 levels lead to increased glutathione synthesis, and hence increased oxidative stress resistance. (*B* and *C*) The increase in *gcs-1* expression associated with loss of PRDX-2 does not result from increased activation of PMK-1 since levels of arsenite-induced PMK-1 activation are *lower* in *prdx-2* (*gk169*) animals than in wild type (N2). Western blot analysis of ≈3 μg of protein extracted from wild-type (N2), *prdx-2* (*gk169*), *pmk-1* (*km25*), and *sek-1* (*km4*) mutant animals, treated with the indicated concentrations of sodium arsenite for 5 min (*B*) or 5.0 mM sodium arsenite for the indicated length of time (*C*), revealed that there were lower levels of phosphorylated PMK-1 in arsenite-treated *prdx-2* (*gk169*) animals compared with wild type (N2). Levels of phosphorylated PMK-1 (PMK-1-P) were determined by using an anti-phospho-p38 antibody, which recognizes only the phosphorylated form of PMK-1. β-Tubulin levels were determined as a loading control. Each assay was performed at least twice and a representative experiment is shown. (*D*) The reduced levels of phosphorylated PMK-1 in the *prdx-2* mutant do not reflect decreased total PMK-1 levels. Western blot analysis of 10 μg of protein extracted from wild-type (N2), *prdx-2* (*gk169*), and *pmk-1* (*km25*) mutant animals with anti-PMK-1 and anti-β-tubulin antibodies (loading control).

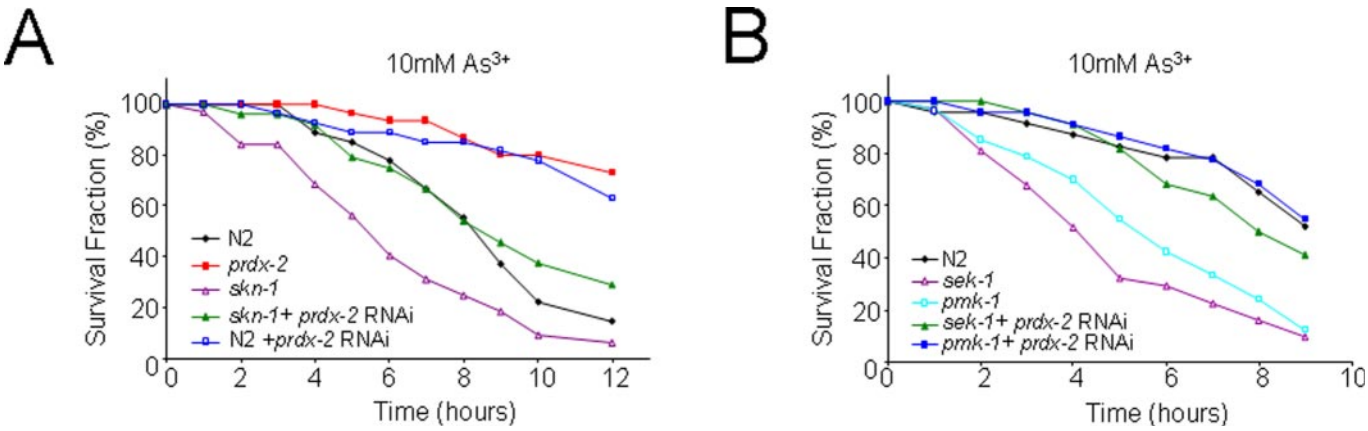


**Fig. S5.** Components of the SEK-1/PMK-1/SKN-1 signaling pathway are not required for the increased arsenite resistance associated with loss of PRDX-2. Loss of PRDX-2 (by microinjection of dsRNA) increases the arsenite resistance of wild-type (N2) animals to levels similar to those of a *prdx-2* (*gk169*) mutant, and also significantly increases the arsenite resistance of the *skn-1* (*zu67*) mutant (*A*) and *pmk-1* (*km25*) and *sek-1* (*km4*) mutant (*B*) animals, suggesting that loss of PRDX-2 can bypass components of the SEK-1/PMK-1/SKN-1 signaling pathway to increase arsenite resistance. [log-rank analysis: N2 vs. N2 + *prdx-2* RNAi ($P < 0.0001$); *skn-1* vs. *skn-1* + *prdx-2* RNAi ($P = 0.004$); *pmk-1* vs. *pmk-1* + *prdx-2* RNAi ($P < 0.0001$); *sek-1* vs. *sek-1* + *prdx-2* RNAi ($P = 0.001$)].

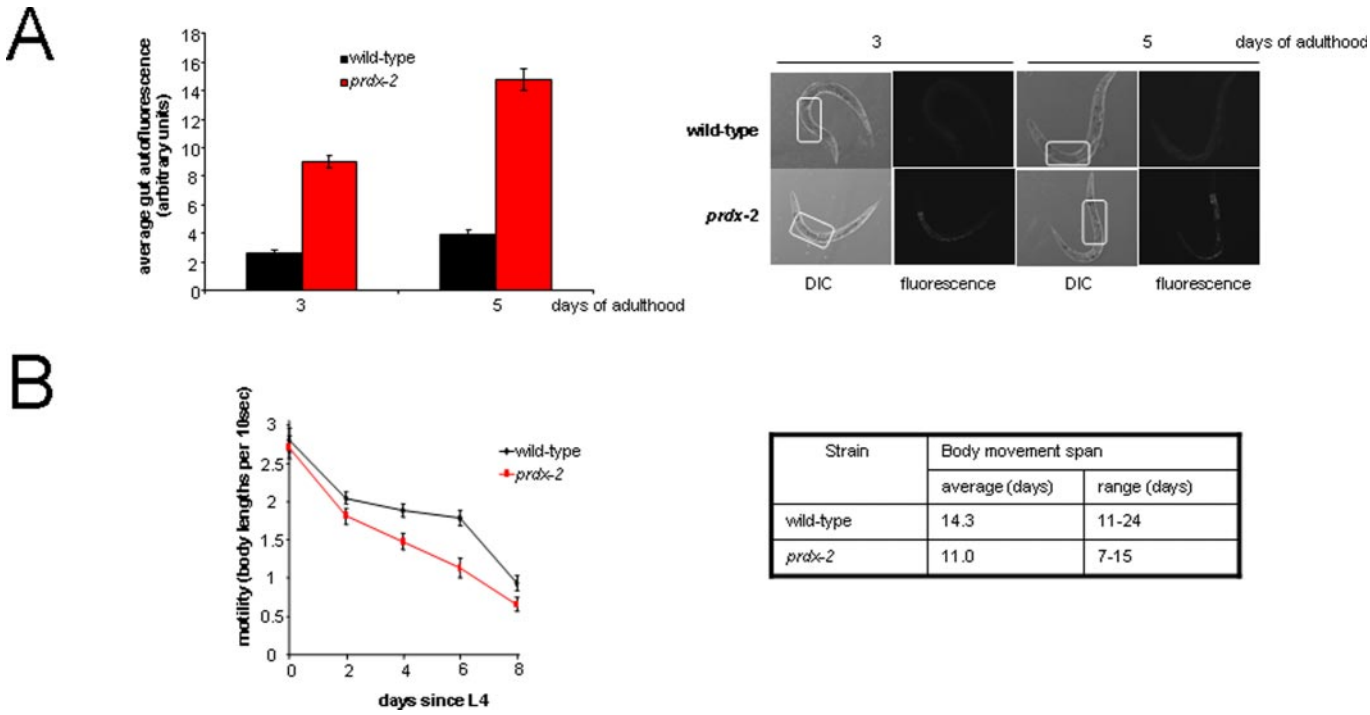


| Strain | Body movement span | |
|---|---|---|
| | average (days) | range (days) |
| wild-type | 14.3 | 11-24 |
| *prdx-2* | 11.0 | 7-15 |

**Fig. S6.** PRDX-2 delays aging. Microscopic observation of synchronized animals maintained at 15 °C on proliferative *E. coli* (OP50) revealed a more rapid accumulation in the gut of the age-associated fluorescent pigment lipofuscin (*A*) and a more rapid decline in motility of *prdx-2* (*gk169*) mutant animals compared with wild-type (N2) (*B*). (*A*) (*Left*) *prdx-2* (*gk169*) animals at 3 and 5 days of adulthood are shown to contain increased levels of lipofuscin (gut autofluorescence) compared with wild-type (N2). Average gut autofluorescence was determined from the anterial gut autofluorescence of 26 or 27 wild-type and *prdx-2* (*gk169*) mutant animals at each time point. Error bars indicate the SEM. (*Right*) Differential interference contrast (DIC) and fluorescent images representative of those images taken at each time point (photographed with identical magnification and exposure) from which gut autofluorescence measurements were made. White boxes indicate (approximately) the region of anterior intestine where autofluorescence was quantified. The reduced size of *prdx-2* mutant animals, previously described by Isermann *et al*. [Isermann K, *et al*. (2004) A peroxiredoxin specifically expressed in two types of pharyngeal neurons is required for normal growth and egg production in *Caenorhabditis elegans*. *J Mol Biol* 338:745–755], is also evident in the DIC image. (*B*) The motility of 35 synchronized wild-type (N2) and *prdx-2* (*gk169*) mutant animals was assessed every 2 days from L4 larval stage. (*Left*) The average motility of wild-type (N2) and *prdx-2* (*gk169*) mutant animals until 8 days after L4 is shown. Error bars indicate the SEM. (*Right*) The average and range in body movement spans are shown.

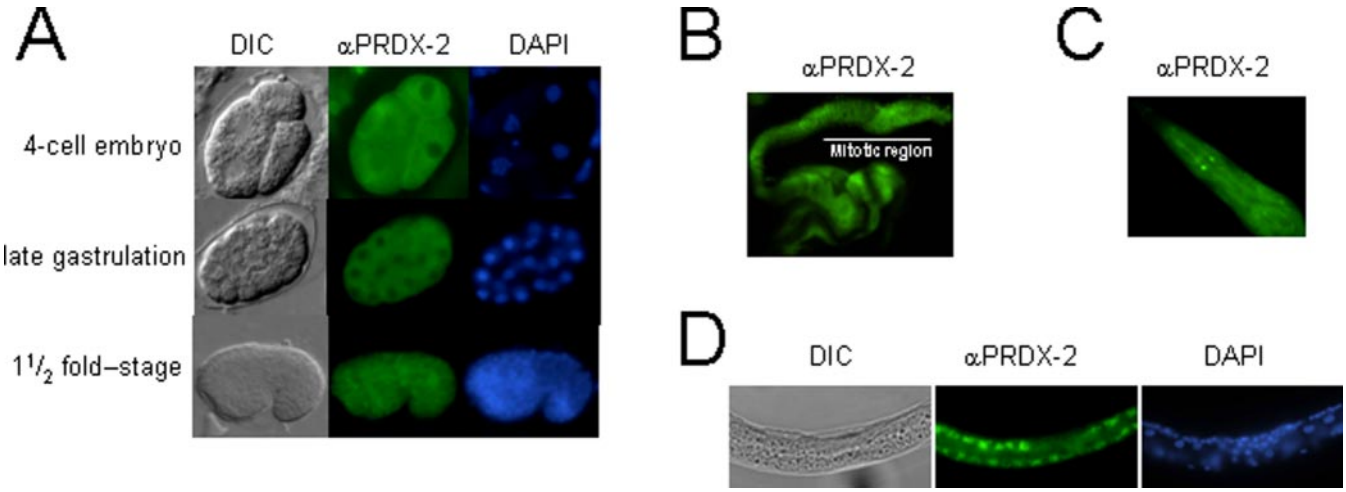


**Fig. S7.** PRDX-2 is widely expressed during embryogenesis and in multiple tissues postembryonically. Immunostaining with anti-PRDX-2 antibodies of wild-type (N2) embryos (*A*), an extruded gonad dissected from an adult hermaphrodite (*B*), and larvae (*C* and *D*) revealed that PRDX-2 is expressed during embryogenesis (*A*) and postembryonically in the gonad (the mitotic region is indicated) (*B*), neurons (*C*), and intestine (*D*). Comparisons with DAPI-stained DNA (*A* and *D*) suggest that PRDX-2 is excluded from the nucleus. Consistent with its activity as a thioredoxin peroxidase, PRDX-2-immunostaining produced a punctate staining pattern in intestinal cells similar to the localization of thioredoxin [Jee C, Vanoaica L, Lee J, Park BJ, Ahnn J (2005) Thioredoxin is related to life span regulation and oxidative stress response in *Caenorhabditis elegans*. *Genes Cells* 10:1203–1210]. Differential interference contrast light images (DIC) are also shown.

**Table S1. Intestinal expression of PRDX-2 does not restore normal fecundity or phase II detoxification gene expression to *prdx-2* mutant animals**

| *C. elegans* strain | Fecundity (brood size) | Relative mRNA levels | |
|---|---|---|---|
| | | *gcs-1* | *gst-7* |
| Wild type (N2) | 194.7 ± 34.8 | 1 | 1 |
| *prdx-2* (*gk169*) | 70.2 ± 12.9 | 2.24 ± 0.64 | 6.87 ± 2.59 |
| *prdx-2* (*gk169*) *Pges-1*::*prdx-2* line 1 | 104.5 ± 17.3 | 2.45 ± 0.59 | 4.07 ± 1.62 |
| *prdx-2* (*gk169*) *Pges-1*::*prdx-2* line 2 | 105.3 ± 18.8 | 2.65 ± 0.77 | 6.48 ± 4.07 |
| *prdx-2* (*gk169*) *Pges-1*::*prdx-2* line 3 | 113.5 ± 13.1 | 1.91 ± 0.62 | 4.53 ± 1.71 |

*prdx-2* (*gk169*) mutant animals have a greatly reduced brood size compared with wild-type (N2) [Isermann K, *et al*. (2004) A peroxiredoxin specifically expressed in two types of pharyngeal neurons is required for normal growth and egg production in *Caenorhabditis elegans*. *J Mol Biol* 338:745–755]. Wild-type fecundity is not restored in any of 3 independently-generated *prdx-2* (*gk169*) lines containing an extrachromosomal array of a transgene expressing PRDX-2 from an intestinal promoter (*Pges-1*::*prdx-2*). Error values (±) indicate standard deviation from the mean brood size for each group of 6 animals. qRT-PCR revealed elevated *gcs-1* and *gst-7* mRNA levels (relative to *act-1* mRNA control) in both *prdx-2* (*gk169*) mutant animals and *prdx-2* (*gk169*) mutant animals expressing PRDX-2 in the intestine (*prdx-2 Pges-1*::*prdx-2* lines 1, 2 and 3) compared with wild-type (N2). Average fold expression of *gcs-1* and *gst-7* relative to wild type (N2) is shown (compiled from multiple independent experiments) and the SEM is indicated (±). Thus, although resistance to hydrogen peroxide is restored to wild-type levels in these same transgenic strains (Fig. 4*C*), phase II detoxification gene expression remains high, indicating that the increased expression of these genes in a *prdx-2* mutant derives from a lack of *prdx-2* expression in tissues outside of the intestine.

**Table S2. Lifespan data for wild-type (N2), *prdx-2* (*gk169*), and wild-type and *prdx-2* (*gk169*) mutant transgenic lines containing extrachromosomal arrays expressing PRDX-2 from an intestinal promoter (*Pges-1*::*prdx-2*) maintained at 15 °C or 20 °C on proliferative or heat-killed *E. coli* OP50**

| *C. elegans* strain | Temp, ° C | Median lifespan, days | Mean lifespan ± SEM, days | *n* | $P^{\dagger}$ | $P^{\ddagger}$ |
|---|---|---|---|---|---|---|
| Wild type (N2) | 20 | 15 | 16.36 ± 0.5 | 110 | — | — |
| *prdx-2* (*gk169*) | 20 | 13 | 13.21 ± 0.3 | 99 | 0.0001(*N*=3) | — |
| Wild type (N2) heat-killed OP50 | 20 | 28 | 26.03 ± 1.0 | 62 | — | — |
| *prdx-2* (*gk169*) heat-killed OP50 | 20 | 14 | 14.10 ± 0.4 | 63 | 0.0001(*N*=2) | — |
| Wild type (N2) | 15 | 19 | 19.09 ± 0.6 | 65 | — | — |
| *prdx-2* (*gk169*) | 15 | 14 | 14.11 ± 0.4 | 84 | 0.0001(*N*=3) | — |
| Wild type (N2) heat-killed OP50 | 15 | 30 | 28.90 ± 0.5 | 115 | — | — |
| *prdx-2* (*gk169*) heat-killed OP50 | 15 | 15 | 15.22 ± 0.4 | 63 | 0.0001(*N*=2) | — |
| Wild type (N2) | 15 | 21 | 20.65 ± 0.4 | 130 | — | 0.0001(*N*=3) |
| *prdx-2* (*gk169*) | 15 | 15 | 15.08 ± 0.4 | 92 | 0.0001(*N*=3) | — |
| N2 *Pges-1*::*prdx-2* line 1 | 15 | 17 | 18.65 ± 0.5 | 80 | 0.893 (*N*=3) | 0.0001(*N*=3) |
| N2 *Pges-1*::*prdx-2* line 2 | 15 | 19 | 19.68 ± 0.7 | 59 | 0.050 (*N*=3) | 0.0001(*N*=3) |
| *prdx-2* (*gk169*) *Pges-1*::*prdx-2* line 1 | 15 | 12 | 12.81 ± 0.4 | 86 | 0.0001(*N*=2) | 0.834 (*N*=2) |
| *prdx-2* (*gk169*) *Pges-1*::*prdx-2* line 2 | 15 | 13 | 13.36 ± 0.4 | 87 | 0.0001(*N*=2) | 0.102 (*N*=2) |
| *prdx-2* (*gk169*) *Pges-1*::*prdx-2* line 3 | 15 | 14 | 14.11 ± 0.4 | 86 | 0.0001(*N*=2) | 0.089 (*N*=2) |

The mean and median lifespan of *prdx-2* (*gk169*) was significantly reduced under all conditions compared with wild-type (N2) maintained under the same conditions. Although *Pges-1*::*prdx-2* restores wild-type levels of hydrogen-peroxide resistance to *prdx-2* (*gk169*) *Pges-1*::*prdx-2* lines (Fig. 4*C*), these lines still have a greatly reduced lifespan compared with wild-type (N2) mutant animals. Moreover, this analysis also shows that, while the presence of *Pges-1*::*prdx-2* transgene in either the wild-type or *prdx-2* mutant backgrounds increases stress resistance above that of the parent strain (Fig. 4 *A–D*), it does not produce any statistically significant effect on lifespan. Mean and median lifespan data are taken from the representative experiments shown graphically in Figs. 3 and 4*E* in which each group contained the indicated number of animals (*n*). Experiments were repeated with similar results. Statistical analysis of differences between the lifespan of different lines maintained under identical conditions was carried out by Cox's regression analysis of multiple (*N*) lifespan experiments.

$^{\dagger}$Compare with N2 under same conditions.

$^{\ddagger}$Compare with *prdx-2*.